

# STARBURSTS VERSUS TRUNCATED STAR FORMATION IN NEARBY CLUSTERS OF GALAXIES

James A. Rose<sup>1</sup>

Department of Physics and Astronomy, University of North Carolina, Chapel Hill, NC 27599

Electronic mail: jim@physics.unc.edu

Alejandro E. Gaba

Department of Physics and Astronomy, University of North Carolina, Chapel Hill, NC 27599

Electronic mail: gaba@physics.unc.edu

Nelson Caldwell<sup>1</sup>

F.L. Whipple Observatory, Smithsonian Institution, Box 97, Amado AZ 85645

Electronic mail: caldwell@fwo99.sao.arizona.edu

Brian Chaboyer<sup>1</sup>

Department of Physics and Astronomy, Dartmouth College, Hanover, NH 03755-3528

Electronic mail: Brian.Chaboyer@Dartmouth.edu

## ABSTRACT

We present long-slit spectroscopy, B and R bandpass imaging, and 21 cm observations of a sample of early-type galaxies in nearby clusters which are known to be either in a star-forming phase or to have had star formation which recently terminated. From the long-slit spectra, obtained with the Blanco 4-m telescope, we find that emission lines in the star-forming cluster galaxies are significantly more centrally concentrated than in a sample of field galaxies. The broadband imaging reveals that two currently star-forming early-type galaxies in the Pegasus I cluster have blue nuclei, again indicating that recent star formation has been concentrated. In contrast, the two galaxies for which star formation has already ended show no central color gradient. The Pegasus I galaxy with the most evident signs of ongoing star formation (NGC7648), exhibits signatures of a tidal encounter. Neutral hydrogen observations of that galaxy with the Arecibo radiotelescope reveal the presence of  $\sim 4 \times 10^8 M_\odot$  of HI. Arecibo observations of other current or recent star-forming early-type galaxies in Pegasus I indicate smaller amounts of gas in one of them, and only upper limits in others.

---

<sup>1</sup>Visiting Astronomer, Cerro Tololo Inter-American Observatory, National Optical Astronomy Observatories, operated by the Association of Universities for Research in Astronomy, Inc., under contract with the National Science Foundation

The observations presented above indicate that NGC7648 in the Pegasus I cluster owes its present star formation episode to some form of tidal interaction. The same may be true for the other galaxies with centralized star formation, but we cannot rule out the possibility that their outer disks have been removed via ram pressure stripping, followed by rapid quenching of star formation in the central region.

*Subject headings:* galaxies: evolution — galaxies: clusters: general — galaxies: elliptical and lenticular, cD — galaxies: interactions — galaxies: starburst — galaxies: intergalactic medium

## 1. Introduction

It is now well-established that the star formation rate (SFR) in rich clusters of galaxies has declined markedly since  $z \sim 0.5$ . Evidence for this decline was first established by Butcher & Oemler (1978, 1984; see Margoniner & de Carvalho 2000 and references therein for recent results), who found a systematic increase in the fraction of blue galaxies in rich clusters with increasing redshift, a phenomenon known as the Butcher-Oemler effect. *HST* images have since shown that the increase in the population of blue galaxies with  $z$  is also accompanied by an increase in the fraction of spiral and interacting/merging galaxies. Thus the decline in SFR in rich clusters since  $z=0.5$  appears connected to the decrease in the population of spirals, and consequent increase in S0's (e.g., Dressler et al. 1997; Poggianti et al. 1999), though the details are complex (Fabricant et al. 2000). The aim of this paper is to better understand what are the driving mechanisms that produce the observed falloff in SFR.

While the basic observation of the Butcher-Oemler effect appears to be generally well-accepted, there is much current debate concerning the causes of the declining SFR, and to what extent the rich cluster environment is involved. On the one hand, the cluster environment is certainly capable of both provoking and quenching star formation in the member galaxies, since both gas removal mechanisms (e.g., Gunn & Gott 1972; Abadi, Moore, & Bower 1999) and tidal perturbations (e.g., Lavery & Henry 1988; Byrd & Valtonen 1990; Moore et al. 1996, 1998; Bekki 1999), which can lead to inward flow of gas and subsequent enhanced star formation, have been proposed.

Evidence for enhanced star formation comes from the discovery of galaxies in distant clusters with strong Balmer absorption lines and no emission lines in their spectra (e.g., Dressler & Gunn 1983). This so-called “E + A” or “K + A” phenomenon is often attributed to the effect of a recent starburst (e.g., Barger et al. 1996), thus indicating that cluster galaxies are ending their star-forming careers in a final burst. Recently, early-type galaxies in *nearby* clusters, such as Coma, with similar K+A spectra have been discovered with surprising frequency by Caldwell et al. (1993) and Caldwell & Rose (1997). Subsequent long-slit spectroscopy (Caldwell et al. 1996) and *HST* imaging (Caldwell, Rose, & Dendy 1999) have indicated that the recent star formation

in these galaxies has been centrally concentrated to the inner  $\sim 2$  kpc in radius. In addition, models of the integrated spectra of some of these systems indicate that the recently terminated star formation was burst-like, not simply a truncation of ongoing star formation (Caldwell et al. 1996; Caldwell & Rose 1998). Thus in these cases the evidence favors a centrally concentrated star formation episode, rather than truncated disk star formation.

On the other hand, the identification of the K+A phenomenon with a starburst episode has been challenged by Newberry, Boroson, & Kirshner (1990) and by Balogh et al. (1999). These authors have pointed out that the distribution of emission line and Balmer line strengths in cluster galaxies does not demonstrably differ from what one might expect for a collection of fading spirals whose star formation was truncated rather suddenly. Furthermore, Balogh et al. (1999) propose that the fraction of K+A galaxies in distant clusters is actually far lower (only about 1% of their sample) than previously indicated, and that there is no indication that the fraction of K+A's exceeds that in the field, nor that the fraction has evolved significantly from  $z=0.5$  to the present epoch. This result, based on the CNOC sample, contrasts strongly with the results of the MORPHS sample, which is reported in Dressler et al. (1999) and Poggianti et al. (1999). One problem is that, except for immediately after a burst episode when the colors are very blue and the Balmer lines are very strongly enhanced, a fading starburst and a fading, truncated disk produce very similar spectra. Thus exceptional care (high signal-to-noise) and fortune are required to distinguish the two. As a result, there is considerable uncertainty as to whether the rather widely assumed poststarburst picture for K+A galaxies is indeed correct, rather than the less dramatic situation of a truncated spiral.

A key unresolved question is the matter of the rapid evolution in SFR since  $z=0.5$ : Is it caused by final large bursts of star formation in cluster galaxies, or is it instead produced by a less dramatic truncation of star formation? Previous efforts to distinguish between the two scenarios in the first question have largely concentrated on interpreting the star formation histories of galaxies through their colors and spectra. However, another way to resolve the issue is by investigating the *spatial distribution of the last star formation* in these galaxies. If the primary effect is simply termination of star formation in an otherwise normal spiral disk, then we would expect to see the fading of a roughly uniformly blue galaxy, with the exception, perhaps, of a redder bulge. If the mechanism is somehow related to starbursts, however, one would expect the fading blue population to be centrally concentrated, since current hypotheses for the production of starbursts all utilize variations on a theme of tidal gravitational perturbations, which cause a pileup of gas in the centers of galaxies, and hence a central starburst.

In this paper we have combined spectroscopic and imaging data of star forming galaxies in nearby clusters to evaluate whether recent star formation in cluster galaxies has been centrally concentrated. We place particular emphasis on the perspective of nearby clusters, since while in distant clusters the processes producing the rapid evolution in SFR are more in evidence, in nearby clusters one can study the processes with higher spatial resolution and higher S/N ratio, both in spectroscopy and imaging. Two datasets relevant to unusual star formation in nearby

clusters are presented in this paper. First, we investigate the spatial distribution of ionized gas in 10 early-type galaxies in nearby rich clusters. We compare the central concentration of the ionized gas with that in an extensive sample of low-redshift field galaxies. The purpose is to evaluate whether or not star formation in the cluster galaxies is unusually centrally concentrated when compared with the field sample. Second, we present B and R images and HI observations of four early-type galaxies in the Pegasus I cluster for which Vigroux et al. (1989) have previously found evidence for ongoing or recently completed star formation. The Pegasus I cluster is particularly relevant here because of its low cluster x-ray emission, which indicates that ram pressure stripping is not a significant process in this cluster. Thus we have an unusual opportunity to isolate the effects of external (tidal) perturbations on the star formation histories in cluster galaxies.

The basic plan for this paper is as follows. In §2 the imaging and spectroscopic data are summarized. In §3 we compare the spatial distribution of ionized gas in early-type galaxies in nearby rich clusters with that of the sample of “field” galaxies. In §4 we discuss radial luminosity profiles, morphology, and  $B - R$  radial color maps of four early-type galaxies in the nearby Pegasus I cluster, as well as 21 cm observations of these galaxies. In §5 we combine the results of the previous sections to assess the nature of the last star formation in cluster galaxies, and place our results in the context of other recent analyses.

## 2. Observational Data

### 2.1. Spectroscopy

Long-slit spectra were obtained of 10 galaxies in three nearby rich clusters. All 10 galaxies were classified to have early-type morphologies by Dressler (1980), but were also known to have emission lines based on previous multi-fiber spectroscopy reported in Caldwell et al. (1993) and Caldwell & Rose (1997). The long-slit spectra of five galaxies in the cluster DC2048-52 and of three galaxies in the double cluster DC0326-53/0329-52 (=A3125/A3128) were obtained with the CTIO 4-meter telescope with the RC spectrograph and Loral 3K x 1K CCD in August 1998. The spectra cover the wavelength region  $\lambda\lambda 5000 - 8000 \text{ \AA}$ , at a dispersion of  $1 \text{ \AA/pixel}$ . Thus the  $\text{H}\alpha$ ,  $[\text{NII}]\lambda\lambda 6548, 6584$ , and  $[\text{SII}]\lambda\lambda 6717, 6731$  emission lines are well centered in these spectra. The scale along the slit direction is  $0.5''/\text{pixel}$ , and the slit width is  $1.7''$ . Exposure times were 20 minutes, with repeat exposures taken in several cases. Two other spectra, of the early-type emission-line galaxies D15 and D45 in the Coma cluster, were obtained with the MMT, and have been previously reported in Caldwell et al. (1996). Briefly, these spectra also cover the same emission lines as the CTIO 4-m spectra, at a dispersion of  $0.8 \text{ \AA/pixel}$ , and a scale along the slit of  $0.3''/\text{pixel}$ .

Since the above long-slit spectra are used in this paper to explore the spatial distribution of star formation in emission-line galaxies in nearby clusters, a reference sample of long-slit spectra of “normal” galaxies is required to use as a benchmark for the cluster galaxies. Recently, Jansen

et al. (2000a,b) have observed a large survey of relatively isolated galaxies, called the Nearby Field Galaxy Survey (NFGS), covering a wide range in absolute magnitude and morphology. In addition to broadband imaging (for luminosity profiles and colors) and globally averaged spectroscopy (for use in comparison with spectroscopy of distant galaxies), they have also obtained long-slit spectra, with the Tillinghast 1.5-m telescope of the F. L. Whipple Observatory, for their entire sample of 198 galaxies. The spectra cover the same [NII], [SII], and H $\alpha$  emission lines as our spectra of the cluster galaxies, at a dispersion of  $\sim$ 1.5 Å/pixel, a slit width of 3'', and a scale along the slit of 2.0''/pixel. Exposure times were typically 15–20 minutes. While the scale along the slit is at four times lower resolution than for the cluster galaxies, the galaxies in the NFGS are typically 2–6 times closer than the cluster galaxies. As a result, after appropriate corrections are made to spatially smooth the NFGS spectra to the same effective seeing as the cluster galaxies, the two samples can be intercompared. It was assumed that the seeing was 1'' for both cluster and NFGS observations. Moreover, the majority of the cluster sample is at a redshift of 14000 km s $^{-1}$ . Thus to bring a galaxy in the NFGS sample to the same effective spatial resolution as the cluster galaxies, a smoothing was applied with a  $\sigma$  of:

$$\sigma^2 = \left(\frac{14000}{4.708V_r}\right)^2 - \left(\frac{1.0}{4.708}\right)^2,$$

where  $V_r$  is the radial velocity of the NFGS galaxy (corrected to the Local Group velocity centroid, as given in Jansen et al. 2000a), and the factor 4.708 accounts for the 2''/pixel binning of the NFGS spectra and the conversion from FWHM to  $\sigma$ .

## 2.2. Imaging of Pegasus I Cluster

Images of four early-type galaxies in the Pegasus I cluster were obtained in the B and R passbands using the 0.9-m telescope at CTIO on the nights of September 3 – 7, 1991. The detector used was a Tektronix 1024<sup>2</sup> pixel CCD. The scale at the focal plane of the 0.9-m telescope is 0.4'' per 24  $\mu$ mm pixel. All observations were taken through thick and variable cloud cover, typically 1 – 2 magnitudes. Thus all color information is on a relative scale. Exposure times were typically 600 seconds each. Multiple exposures were recorded in both B and R for all four galaxies, but due to the variable cloud cover, the S/N ratio in the images varied greatly from one exposure to the next. Thus for most galaxies, a single exposure in each filter typically contained the most information. The seeing ranged from 1.4'' to 2.0'' FWHM, with the seeing in the R passband slightly better than in B.

Analysis of the images was accomplished using the IRAF package. After the frames were trimmed, bias-subtracted, and flat-fielded, a majority of the cosmic rays in each image was removed using the 'cosmicrays' routine. The remaining cosmic rays in the vicinity of the galaxy were removed manually using the 'imedit' routine. An average value of the sky was evaluated from statistics in sky-free zones well away from the galaxy. The task 'ellipse' in IRAF was then

used to obtain isophote fits for each galaxy from the sky-subtracted images. Radial luminosity profiles could then be plotted from the isophote fits. In addition, a model of the isophote fit was constructed using the routine 'bmodel'. This fit was subtracted from the original galaxy image, to look for fine structure in the image where the luminosity gradient is steep.

To produce color maps of the galaxies all selected B and R images of each object were registered by selecting reference stars in the individual frames and using the 'imalign' routine to determine centering offsets. The image quality on each frame was then determined using 'fifpsf' on selected stars in each of the registered frames and averaging the calculated FWHM's. In general, the better seeing R frames had to be degraded to match the seeing on the B frames. This was done by gaussian-smoothing the R frames. To obtain the radial color profile, the final B and R images were fit using 'ellipse' (see above), and the color profile was then determined from a point-to-point subtraction of these profiles in magnitude form. Two types of errors have been considered for the luminosity and color profiles. Statistical errors for the magnitudes were calculated by the 'ellipse' task from the rms scatter of intensity data along the fitted ellipse. We also separately calculated the error in the magnitudes based on estimated uncertainties in the sky subtraction, which dominates the errors at large radial distances from the galaxy centers. Specifically, we assumed a 1% error in the sky background. Both error estimates have been plotted on the luminosity and color profiles.

### 2.3. HI Observations of Pegasus I

Neutral hydrogen observations in the 21 cm transition were obtained for the four early-type galaxies in the Pegasus I cluster that were also imaged in B and R. The observations were acquired on July 14-15, 1999 using the 305-m Arecibo radiotelescope of the National Astronomy and Ionosphere Center<sup>2</sup>. The L-narrow receiver was used at the upgraded Gregorian feed. All four subcorrelators covered a frequency range of 25 MHz with 1024 spectral channels (at  $5 \text{ km s}^{-1}$  resolution), centered at 1403 MHz (i.e., centered at a redshift of  $3675 \text{ km s}^{-1}$ ), and observations were recorded in both circular polarizations. The system temperature was approximately 30 K, and the gain  $\sim 10 \text{ K/Jy}$ . The observations consisted of sets of five minute on-source and five minute off-source integrations ("scans"). Each five minute observation actually consisted of a series of five one minute integrations ("dumps"), with each one minute observation separately recorded. For NGC7557, NGC7611, NGC7617, and NGC7648, the total number of five-minute scans is 5, 4, 6, and 5 respectively. Hence, for instance, 25 minutes of integration were carried out for NGC7648 on-source, and 25 minutes off-source.

The 21 cm data were reduced using the Analyz software at Arecibo. As a first step, all 5 on

---

<sup>2</sup>The National Astronomy and Ionosphere Center is operated by Cornell University under a cooperative agreement with the National Aeronautics and Space Administration

and off dumps of each scan were added together. Then an ON/OFF-1 spectrum was obtained, to subtract the background and normalize the spectrum to the correlator response, thereby yielding percent of system temperature vs. frequency. The frequency was then converted to heliocentric velocity. The system temperature was corrected for gain versus zenith angle and temperature versus zenith angle dependencies, using available calibration curves, and converted to flux in Janskys. An average spectrum for each galaxy was obtained by averaging the ON/OFF-1 spectra of all 5 minute scans. Finally, the baseline for each averaged spectrum was fit by a polynomial and subtracted. For the two detected galaxies the integrated 21 cm flux in  $\text{Jy km s}^{-1}$  was obtained. The total flux was converted to HI content in solar masses using the relation found in, e.g., Binney & Merrifield (1998)

$$\frac{M_{HI}}{M_{\odot}} = 2.356 \times 10^5 \left( \frac{D}{\text{Mpc}} \right)^2 \frac{\int_{-\infty}^{\infty} S(v) dv}{\text{Jy km s}^{-1}},$$

where  $D$  is the distance to the galaxy and  $S(v)$  is the flux in Jy as a function of velocity.

Using the absolute magnitudes in the B band given in Vigroux, Boulade, & Rose (1989), we calculated the total B band luminosity for each galaxy. We then formed the HI mass to B band luminosity ratio, in solar units.

For the non-detected galaxies upper limits limits were calculated in the following manner. The flux in  $400 \text{ km s}^{-1}$  wide bandpasses (the expected velocity widths for the galaxies) were integrated from one side of the baseline-subtracted spectrum to the other, centered at 200 km/s intervals. The mean and standard deviation of the distribution were calculated and the upper limit taken at the  $3\sigma$  level. We also took the rms of the baseline-subtracted spectrum, multiplied by the square root of the number of channels in the above velocity passband, and used 3 times this value as another estimate of the  $3\sigma$  upper limit. In most cases the two estimates agreed closely, but in a few cases, where the noise in the spectra contained structure (due to radio frequency interference and standing waves from the Sun in observations taken near sunrise), we considered the first method to provide a more conservative upper limit.

### 3. Emission-Line Early-Type Galaxies in Nearby Clusters

Having discussed the new observations, we now employ that data to establish the centrally concentrated nature of star formation in our cluster galaxies.

As was mentioned in §1, multi-fiber spectroscopy of early-type galaxies in five nearby rich clusters has revealed that  $\sim 15\%$  of these galaxies have experienced an unusual star formation history in the recent past (Caldwell et al. 1993; Caldwell & Rose 1997). Since the galaxies studied have been classified as E or S0 or S0/a by Dressler (1980) on high-quality photographic plates, *any* recent star formation is in principle unusual. In fact, (particularly in the SW region of the Coma cluster) many of these galaxies have unusual star formation histories, regardless of morphology.

That is, they exhibit the K+A pattern of strong Balmer absorption lines but no emission, along with relatively red colors, that is characteristic of galaxies which have recently completed star formation, whether in a burst or through sudden truncation of ongoing star formation. Since K+A galaxies are rare in the field at the present epoch, for *any* morphological type, we can indeed conclude that the cluster K+A's are unusual.

The situation of cluster early-type galaxies with *current* star formation, as evidenced by emission spectra characteristic of HII regions, is less certain. Elliptical and S0 galaxies in the field with ongoing star formation are rare. For example, 44 galaxies in the NFGS within the absolute magnitude range  $-17.4 > M_B > -22.0$  are classified as early-type (i.e., with morphological type parameter  $T \leq 0$ ). Of these, 22 are not detected in emission, 19 have nuclear emission that is dominated by an active galactic nucleus<sup>3</sup> (AGN), and only 3 have nuclear emission dominated by star formation. The latter 3 galaxies, A11352+3536, A12001+6439, and A22551+1931N, have been categorized as a Markarian blue compact dwarf, a blue compact dwarf, and a “multiple galaxy” respectively (as reported in NED), and hence are unusual for their early-type classifications. Thus in principle, the early-type emission-line galaxies found in clusters are truly experiencing unusual star formation. *However, one must also consider the possibility that these galaxies are simply misclassified spirals, in which case ongoing star formation is to be expected.*

Large errors in morphological classification (viz., confusing a spiral galaxy for an E or S0) appear unlikely at the distance of the Coma cluster. In Fig. 1 we compare V band images of the two current star forming (CSF) early-type galaxies D15 and D45 with several of the blue disk galaxies in Coma studied by Bothun & Dressler (1986; hereafter BD86). All images are 400 second exposures taken with the 1.2-m telescope at the F. L. Whipple Observatory. As can be seen from Fig. 1, the disks of D15 and D45 are quiescent in comparison with those of the BD86 spirals. However, high resolution images with WFPC2 on *HST* reveals that what appears to be the central “bulges” of D15 and D45 are actually bright star-forming regions, unresolved on the ground-based images (Caldwell, Rose, & Dendy 1999). Thus, while the “bulges” of D15 and D45 have in fact been misunderstood from the ground, the *HST* images reinforce the idea that D15 and D45 have had star formation quite unlike a normal spiral, in that the star formation is highly centrally concentrated.

On the other hand, two of the best-studied clusters, DC2048-52 and DC0326-53/0329-52, are at twice and 2.5 times the distance of Coma, respectively. One might question whether at this distance the ground-based morphological distinctions between early-type and late-type galaxies are reliable. If, in fact, the emission-line galaxies in the clusters are simply misclassified spirals (and thus not unusual at all), then the spatial distribution of the star formation should be similar to that in “normal” spirals, i.e., spread throughout the disk. To evaluate this “misclassified

---

<sup>3</sup>We use the emission-line ratio  $[\text{NII}] \lambda 6584 / \text{H}\alpha > 0.5$  as a dividing line between AGN/LINER spectra and HII region/star formation spectra, and when available,  $[\text{OIII}] \lambda 5007 / \text{H}\beta > 0.5$ . This dividing line is based on the distribution of AGN, LINERs, and HII regions in Fig. 5 of Baldwin, Phillips, & Terlevich (1981).

spiral” hypothesis, we have used the long-slit spectra described in §2, in comparing the spatial distribution of emission lines in the cluster galaxies to that in the NFGS sample.

To make a quantitative comparison of the emission line distributions in field and cluster galaxies, we have defined a measure for the central concentration of emission lines. For most of the galaxies, the emission along the slit is smooth enough that we simply measure the H $\alpha$  flux in the nuclear pixel and in the pixels on both sides of the nucleus that are closest to the effective radius, where  $r_{eff}$  is taken from Jansen et al. (2000a). We define the quantity C/R to be the ratio of the H $\alpha$  flux in the central pixel to the average H $\alpha$  flux in the two pixels on either side of the nucleus at  $r_{eff}$ . However, for some of the NFGS galaxies the emission is so concentrated into discrete knots that the emission right at  $r_{eff}$  can be very low, or undetected. In those cases, we use the alternative ratio C/B, which is the ratio of the nuclear H $\alpha$  flux to the average flux in the two brightest extranuclear knots.

The cluster galaxies in DC2048-52 and DC0326-53/0329-52 have a typical absolute blue magnitude of -19 (where we have adopted a Hubble Constant of  $H_0 = 70 \text{ km s}^{-1} \text{ Mpc}^{-1}$ ). The NFGS, by design, covers a very large range in absolute magnitude. To avoid the behavior exhibited by the extreme bright and faint ends of the galaxy luminosity function, we restrict our analysis of the NFGS to the magnitude range  $-17.4 > M_B > -22.0$ . In addition, since the emission lines in our cluster galaxies have characteristic HII region line intensity ratios, thus indicating star formation rather than an AGN, we avoid those galaxies in the NFGS whose nuclear spectra are dominated by an AGN (whether Seyfert or LINER). In the one case among the cluster galaxies in which an AGN spectrum dominates in the nucleus (D15 in Coma), we measure only the narrow-line component of the H $\alpha$  emission. Altogether, we measure C/R and C/B indices for 66 galaxies in the NFGS, excluding the 33 that are dominated by an AGN spectrum. The remainder of the sample falls outside the absolute blue magnitude limits, or has unmeasureably low H $\alpha$  emission. We also measure the same indices in our sample of 5 galaxies in DC2048-52, 3 galaxies in DC0326-53/DC0329-52, and two galaxies in Coma. Results for the 66 NFGS galaxies and for the 10 cluster galaxies are given in Tables 1 and 2 respectively, where the morphological type, absolute blue magnitude and effective radius is listed for each galaxy, along with the C/R or C/B index. The default is the C/R index, i.e., the C/B index is only listed when the emission is highly resolved into knots.

To compare the central concentration of the emission in the cluster versus the NFGS galaxies, we have plotted histograms of the C/R indices for both the cluster sample and for the subsample of the NFGS described above. We again emphasize that the NFGS galaxies satisfying these criteria consist almost entirely of spirals, since early-type galaxies which have emission are almost exclusively of the AGN variety. Since the point of our comparison is to assess whether the star-forming cluster galaxies might be misclassified spirals, it is in fact appropriate that the restricted NFGS be largely comprised of spirals. The two histograms are compared in Fig. 2, where the upper histogram is for the cluster galaxies. For the NFGS galaxies in the lower histogram we have shaded those galaxies which have been classified (based on information given

in NED) as Markarian, starburst, interacting, double, or blue compact dwarf. Note that for both histograms, we have binned all values of  $C/R > 10$  into a single bin at 10. The two distributions are clearly different, in that the majority of the NFGS galaxies have  $C/R < 2.0$ , while all of the cluster galaxies have  $C/R > 2.0$ . On the other hand, the distribution of shaded galaxies in the NFGS histogram is quite similar to that of the cluster galaxies. To quantify these assertions we have applied the Kolmogorov-Smirnoff two-sample test. In particular, the likelihood that the cluster sample and the NFGS are drawn from the same parent population is only  $9.4 \times 10^{-5}$ . On the other hand, the likelihood that the shaded NFGS and the cluster sample are drawn from the same parent sample is 0.45, while the likelihood that the shaded NFGS and the remainder of the NFGS are drawn from the same population is only  $5.1 \times 10^{-4}$ . In short, the starforming early-type cluster galaxies have more centrally concentrated emission than do typical field galaxies.

An additional impression of the differences in emission profiles between the cluster sample and NFGS can be gained from examination of Figs. 3 - 5, where the long-slit spectra of galaxies with various ranges in  $C/R$  ratios are shown. Specifically, the NFGS has been divided into intervals of low concentration ( $C/R < 2.0$ ), intermediate concentration ( $2.0 \leq C/R \leq 4.0$ ), and high concentration ( $C/R > 4.0$ ). Representative spectra of NFGS galaxies from these three classes are reproduced in Fig. 3. The corresponding intermediate and high concentration long-slit spectra of the cluster galaxies are presented in Figs. 4 and 5; there are no low concentration cluster galaxies in our sample of 10 objects.

In conclusion, early-type galaxies in nearby clusters with current star formation, as evidenced by emission lines with  $[\text{NII}]/\text{H}\alpha$  characteristic of HII regions, have unusually centrally concentrated emission, when compared to a sample of relatively isolated galaxies. In addition, many of the small ( $\sim 20\%$ ) fraction of field galaxies which do have emission as centrally concentrated as the early-type galaxies in clusters are known as starburst and/or Markarian or blue compact dwarf galaxies. This further underscores our principle conclusion that the cluster early-type galaxies are experiencing unusual star formation, i.e., are not normal spirals that have been misclassified as early-type galaxies. In addition, the unusual (central) location of the star formation suggests that it has been concentrated into a burst.

#### 4. The Pegasus I Cluster and its Unusual Early-Type Galaxies

We now move on to discuss imaging of four early-type galaxies, with ongoing or recent star formation, in a nearby cluster to further assess the nature of star formation episodes in early-type galaxies.

As briefly mentioned in §1, the Pegasus I cluster is a nearby cluster of galaxies having a low velocity dispersion, no detected x-ray emission, and no evidence for systematic depletion of HI in its spiral galaxies (Giovanelli & Haynes 1986). These facts taken together indicate that ram pressure stripping cannot play an important role in the evolution of galaxies in Pegasus I, so that

unusual evolutionary events in the cluster must be attributed to other causes. Consequently, Pegasus I represents a relatively low-density cluster environment for investigating the triggering mechanism of star formation in cluster galaxies. This investigation could also shed light on the presence of field K+A galaxies.

Based on the presence of enhanced Balmer absorption lines and/or emission, Vigroux et al. (1989) found that four Pegasus I early-type galaxies show evidence for ongoing or recently completed star formation activity.<sup>4</sup> These four early-type galaxies have unusual star formation histories for early-type galaxies, and hence are good candidates for further study in regard to the mechanism that triggers star formation in cluster galaxies.

To clarify the nature of the recent star formation, we obtained B and R passband CCD images of the four galaxies. The observations are described in §2. In what follows we address two primary questions from the Pegasus I imaging data. First, what can we deduce about the spatial distribution of the latest star formation in the four galaxies? Does it appear to have been widespread, or perhaps centrally concentrated? Second, is there evidence for morphological disturbances in the galaxies which could be associated with the recent star formation? The first question is most directly addressed from examination of the radial color (and luminosity) distributions, while the second question is best evaluated from the appearance of the broadband images. Here we also address a third question through the Arecibo 21 cm observations, namely, whether gas is still resident in the galaxies after the last star formation was completed.

#### 4.1. Radial Luminosity and Color Profiles

We begin with an analysis of the radial surface brightness and color profiles for the four galaxies, which are plotted in Fig. 6. The azimuthally-averaged radial surface brightness profiles are plotted both as a function of radius,  $r$ , and  $r^{1/4}$ , to aid in assessing the contributions of disk and bulge. In the case of NGC7648 a pure  $r^{1/4}$  law appears to fit the observed luminosity profile satisfactorily at all radii, except for a mild inflection at  $\sim 1.5$  in  $r^{1/4}$ , ( $\sim 5''$ ). However, for the other three galaxies, departures from the  $r^{1/4}$  law are clearly evident in the outer parts of the profiles, thus indicating that these galaxies have disks.

We now turn to the radial color profiles. Two of the galaxies, NGC7617 and NGC7648, show unusual color gradients in the sense that they become redder with increasing distance from

---

<sup>4</sup>There were originally five such galaxies, but it later became evident that one of the five unusual galaxies, namely NGC7583, has been misidentified. Another galaxy, NGC7604, which is an asymmetric spiral, is incorrectly called NGC7583 in the Catalog of Galaxies and Clusters of Galaxies (Zwicky et al. 1961). The incorrect coordinates are also published in Chincarini & Rood (1976), and were used by Vigroux et al. (1989). The real NGC7583 is a background galaxy, at a redshift of  $12610 \text{ km s}^{-1}$ , as clarified in NED. Thus the strong emission lines and enhanced Balmer absorption reported by Vigroux et al. (1989) for NGC7583 are not necessarily unusual, since they actually refer to the spiral galaxy NGC7604 in Pegasus I.

the nucleus. Such behavior is the reverse of the general blueward color trend with increasing radius exhibited by most E/S0 galaxies (a typical early-type galaxy of their luminosity has a color gradient of  $\Delta(B-R)/\Delta(\log r) \sim -0.1$ , e.g., Vader et al. 1988; Peletier et al. 1990; Balcells & Peletier 1994). Specifically, the radial color profile of NGC7617 shows a steady reddening from  $\sim 2''$  (i.e., the seeing limit) to  $\sim 15''$ , by slightly more than 0.2 mag in  $B-R$ , while in NGC7648 the nucleus is 0.5 mags bluer than at a radius of  $10''$ . In NGC7617 the enhanced Balmer absorption lines are accompanied by  $[\text{OII}]\lambda 3727$  emission, indicating that star formation is still ongoing. In the case of NGC7648, the emission is considerably stronger, indicating that this galaxy is in the midst of a star formation episode. In contrast, NGC7557 and NGC7611 have flat radial color distributions within the uncertainties; these two galaxies have true “K+A” spectra in the sense that enhanced Balmer absorption lines are seen, but no detectable emission. To summarize, a very blue central region is seen in the case where a starburst is in progress (NGC7648), a less dramatically blue nucleus is evident in the case where ongoing star formation is less pronounced (NGC7617), and no color gradient is present in the two cases where there has been recent, but no longer ongoing, star formation (NGC7557 and NGC7611).

#### 4.2. Morphologies

The morphologies of the four galaxies provide an additional perspective. While the two true “K+A” galaxies NGC7557 and NGC7611 show little morphological peculiarity, NGC7617 has a long curving dust lane, and NGC7648 shows a variety of interesting features. In Fig. 7(a), which is a B bandpass image of NGC7648, an asymmetric nucleus is visible, along with a luminous arc centered  $2.5''$  to the NW of the galaxy center. A second arc curves from the eastern end of the first arc to a knot  $6''$  E of the nucleus. The second arc is also visible in Fig. 7(b), which is taken from an R band image, at a factor of two smaller scale. At lower surface brightness levels, i.e., outside  $10''$  in radius, faint ripples can be discerned. The faintest ripples are better seen in Fig. 7(c), which is the same R band image displayed at a different contrast level. The fine structure features are perhaps best displayed in the difference image between the sky-subtracted frame and the model frame created from the ellipse fitting (cf., §2), which is shown in Fig. 7(d). The asymmetric morphological features discussed above are characteristic of disturbances found in the late stages of a major (i.e., roughly equal-mass) merger, such as NGC3921 (Schweizer 1996 and private communication).

In contrast, both NGC7557 and NGC7611 show only minor morphological peculiarities. There is faint outer spiral structure in NGC7557, as seen in Fig. 8. NGC7611 has a bright bulge and a faint disk, which are seen in 9(a). In the “fine structure” image, obtained by subtracting the model fit from the original R band image, it can be seen (in 9(b)) that elliptical isophotes provide a poor fit to the light distribution inside the central  $\sim 3''$ , where a number of darker and brighter regions can be seen. The centermost bright and dark features are artifacts caused by the few saturated pixels in this image. However, the saturated pixels do not affect the model fitting, and

the isophotal deviations are apparent as well on the model-subtracted unsaturated image in 9(a), only are not as visible as in the better exposed image. The bilateral symmetry of the isophotal deviations suggests a boxy structure in the nucleus, which is not uncommon in early-type galaxies (e.g., Bender, Döbereiner, & Möllenhoff 1988). In NGC7617 the above-mentioned dust lane, which extends for about 45° from NW to N, can be seen in both B and R images, which are displayed in Fig. 10(a) and (b).

#### 4.3. 21 cm Results

The HI content of the Pegasus galaxies should also give us clues as to the origin of their most recent (or ongoing) star formation. NGC7648 and NGC7617 are both detected in HI at their previously known optical velocities, at the  $10\sigma$  and  $6\sigma$  levels respectively, while NGC7611 and NGC7557 are not. The continuum-removed spectra for NGC7648 and NGC7617 are plotted in Fig. 11. Assuming a distance of 60 Mpc to Pegasus I, we find a  $3\sigma$  upper limit of  $1 \times 10^8 M_\odot$  and  $2 \times 10^8 M_\odot$  for NGC7611 and NGC7557 respectively (cf. §2 for a discussion of how the upper limits were determined). On the other hand, the total HI masses in NGC7648 and NGC7617 are  $\sim 4 \times 10^8 M_\odot$  and  $2 \times 10^8 M_\odot$  respectively. Data on the HI detections and upper limits for the Pegasus I galaxies are summarized in Table 3. Upon inspection of the 21 cm profiles, it is evident that NGC7617 exhibits a flat profile, characteristic of a rotating disk, while NGC7648 shows a predominantly peaked profile, which is expected if much of the remaining HI has been funneled into the central region. Due to the relatively high levels of time-variable RFI that occurred during the NGC7648 observations, which were taken near sunrise, it is difficult to assess the reality of the velocity features on either side of the main peak in the profile of NGC7648. If real, they indicate the presence of higher velocity material that may be distributed at larger radius in a rotating disk.

#### 4.4. NGC7648

From the above discussion it is evident that NGC7648 offers a promising opportunity to explore the properties of an early-type galaxy in a nearby cluster that is undergoing a central starburst. Here we compare the observed properties of NGC7648 to those of several well-studied galaxies considered to be prototypical cases of late-stage mergers. Specifically, we consider NGC3921 and NGC7252, both of which are considered to be late-stage mergers of nearly equal mass disk galaxies (Schweizer 1996; 1982), and NGC2782 and NGC4424, which are suspected to be late-stage mergers involving an intermediate (4:1) mass ratio (Smith 1994; Kenney et al. 1996).

The principal characteristics of the above galaxies are summarized in Table 4, where all observations taken from the literature have been placed on a common Hubble constant of  $H_0 = 70 \text{ km s}^{-1} \text{ Mpc}^{-1}$ . A common theme for these late stage mergers is the presence of substantial atomic hydrogen in the *outer regions* of the galaxies, i.e., typically associated with the stellar tidal tails

(e.g., Hibbard et al. 1994; Jogee, Kenney, & Smith 1999). In contrast, the molecular gas tends to be confined to the main bodies of the galaxies (Hibbard et al. 1994; Jogee, Kenney, & Smith 1999), and the ionized gas, as represented by  $\text{H}\alpha$  emission, tends to be very centrally concentrated. An  $r^{1/4}$  profile and prominent tidal tails are evident in roughly equal mass mergers, while the appearance of an exponential profile and lack of tidal tails are characteristic of intermediate mass ratio mergers. In general, the mergers show concentrated ongoing star formation, as evidenced by strong Balmer absorption lines (e.g., Fritze-von Alvensleben & Gerhard 1994 for NGC7252; Schweizer 1996 for NGC3921), and large far-infrared (FIR) luminosities.

NGC7648 does share some of the key characteristics of late-stage mergers, beyond the morphological knots and ripples discussed in §4.2. In particular, the FIR luminosity and colors, radio power, and optical emission and absorption spectrum are all indicative of a burst of star formation. However, NGC7648 shows puzzling departures from the prototypical merger cases summarized in Table 4. While no tidal tails are evident in NGC7648, which is a characteristic of the two intermediate mass ratio merger candidates, current data appears to favor an  $r^{1/4}$  law profile (although a deeper image is clearly needed). A pure  $r^{1/4}$  law profile is expected from an equal mass merger, in which violent relaxation has played a strong role. Furthermore, while NGC7648 does show an elevated star formation level, the HI content of the galaxy is very low. In addition, although there is no direct information regarding the spatial distribution of the atomic hydrogen, the peaked HI profile from the Arecibo observations suggests a centrally concentrated distribution. Unfortunately, there is no data concerning the molecular gas content of NGC7648. Overall, no clearcut picture emerges as to how to place NGC7648 within the context of late-stage mergers. We examine the implications of this comparison in §5.3.

#### 4.5. Summary

Given the variety of data presented in this section, we briefly summarize the primary results before going on in §5 to examine the implications of both the long-slit spectroscopy of §3 and the Pegasus I results. The main conclusion to be drawn from the Pegasus I data is that in two of the four galaxies with ongoing or recent star formation, the central  $\sim 1$  kpc in radius is substantially bluer than the surrounding disk. Since color gradients in early-type galaxies tend to run in the opposite direction, we consider the bluer centers to provide conclusive evidence that the latest star formation has been centrally concentrated in those two galaxies. This is especially true for the one case where star formation is still very active, NGC7648. *Here the evidence is clear that a nuclear starburst is actually in progress, as opposed to the truncation of disk star formation.* Thus our results on NGC7617 and NGC7648 in Pegasus I are in accord with those for the cluster emission-line galaxies in §3, namely, some galaxies in nearby clusters are currently undergoing star formation that is completely unlike disk star formation in a normal spiral galaxy. The overall resemblance of the morphological irregularities found in NGC7648 to that of late stage “field” merger systems, as well as the centralized star formation, suggests that NGC7648 is the result of

some kind of merger, though other possibilities remain, as is mentioned in §5.3.

The situation regarding the two K+A galaxies, NGC7557 and NGC7611, is unclear because neither of these galaxies has a blue nuclear region (although we note that a fading centrally concentrated starburst would rapidly tend not to have a noticeable color gradient). Long slit spectra showing the Balmer absorption lines (a more sensitive diagnostic than broadband color gradients) are needed to sort out whether these two also had centrally located star formation. Whatever the case, ram pressure stripping is not a candidate for causing the unusual star formation history in the Pegasus I galaxies.

## 5. Discussion

To summarize, two principal results have been obtained. First, long-slit spectroscopy of emission-line galaxies in the Coma, DC2048-52, and DC0326-53/DC0329-52 nearby rich clusters has demonstrated that centralized (in comparison to a field galaxy sample) episodes of star formation occur in galaxies inhabiting the cluster environment at the present epoch. Second, we have found, on the basis of B and R imaging (viz., the presence of reverse color gradients in their central regions), that centralized star formation is also occurring in galaxies in the Pegasus I cluster. The key point regarding the Pegasus I cluster is that it represents a mild cluster environment in which ram pressure stripping is unlikely to be a factor. We now elaborate on these two results, placing them into context with other research on the evolution of galaxies in clusters.

### 5.1. Starbursts versus Truncated Star Formation

A number of recent investigations have addressed the issue of whether star formation in cluster galaxies primarily ends through rapid truncation or through a major starburst, a question that has been debated for some time (e.g., Newberry, Boroson, & Kirshner 1990). Specifically, studies of the color-magnitude relations of galaxies in relatively distant clusters (e.g., Kodama & Bower 2000), as well as the statistics of emission line equivalent widths (e.g., Balogh et al. 1997), indicate that many, if not most, of the galaxies are losing their gas through a truncation of disk star formation, rather than via a major outburst of star formation. However, the evidence presented here, along with the evidence of centralized star formation in cluster galaxies already published in Caldwell et al. (1996) and Caldwell, Rose, & Dendy (1999), demonstrates that in at least some cluster galaxies, centralized episodes of star formation have taken place which are very different from “normal” star formation in a disk. Thus some mechanism must be sought that either drives gas to the central regions of galaxies and provokes star formation there, or that selectively removes gas from the outside and then produces a terminal episode in the center. As is discussed in §5.2 below, in the Pegasus I cluster the evidence points quite clearly in the direction of a tidally induced star formation episode rather than gas removal by ram pressure. Thus the cluster environment is

capable of producing both truncated star formation and enhanced centralized outbreaks as well. It is natural to suspect, therefore, that both evolutionary mechanisms are important in clusters.

To place the evidence for centralized star formation found here within the context of other work, we mention two other results which may be related. Koopmann & Kenney (1998) have emphasized the peculiar aspects of the morphologies of spirals in the Virgo cluster. In particular, they discuss a class of “truncated” spirals (which they refer to as morphological type St), that have nuclear emission and central light concentrations typical of late-type spirals, but quiescent disks that are usually associated with early-type spirals. Hence the Virgo St spirals, which have centrally concentrated emission, may be analogs to the early-type galaxies with emission that we are finding in other, more distant, clusters. In addition, Moss & Whittle (1993, 2000) have found large numbers of spiral galaxies in 8 nearby clusters which have “circumnuclear” (i.e., centrally concentrated) emission. Moreover, the spirals with circumnuclear emission are associated with morphologies indicative of tidal interaction. Thus it appears likely that our cluster emission-line galaxies have much in common with those of Moss & Whittle.

## 5.2. Tidal Disturbances versus Ram Pressure Stripping

Our second result, obtained from the Pegasus I cluster, addresses the role of gas stripping versus tidal interaction in driving galaxy evolution in clusters. Various lines of evidence (cf., discussion in §1) have convincingly demonstrated the importance of ram pressure stripping in depleting the gas reservoirs in galaxies in the rich cluster environment. The primary observational evidence for ram pressure stripping *in action* comes from studies such as Gavazzi et al. (1995) and Kenney & Koopmann (1999), where the radio and optical morphologies show that star formation is preferentially occurring in an asymmetric extranuclear arc. The inference is that star formation is induced at the interface between the leading edge of the infalling galaxy and the hot cluster ICM. The observational signatures have now been modelled by Quilis, Moore, & Bower (2000), whose 3-d gas dynamical simulations also show the characteristic bow shock effect. On the other hand, in the mild environment of the Pegasus I cluster, ram pressure stripping cannot plausibly be a factor, and yet two early-type galaxies are found with ongoing centralized star formation. In addition, the morphology of the most clearcut star forming case in Pegasus I, NGC7648, is different from those of the three galaxies in A1367 which are believed to be in dynamical interaction with the cluster ICM. While the morphology of NGC7648 is complex, there is no sign of a preferential edge (bow shock) to the star formation. Rather, non-spiral disturbances are concentrated into knots and perhaps ripples, which are suggestive of tidal interaction. Thus our second result is that tidal disturbances do indeed play an important role in triggering star formation episodes in the cluster environment.

Evidence for the role of tidal disturbances in clusters has been presented in several previous studies. Rubin, Waterman, & Kenney (1999) have demonstrated that approximately half of the spiral galaxies in the Virgo cluster have disturbed rotation curves. While they argue that

the disturbances are likely to be tidal in nature, they do not distinguish between galaxy-galaxy and galaxy-(sub)cluster interactions. A specific example of an early-type Virgo spiral believed to be a late-stage merger remnant is NGC4424 (Kenney et al. 1996). Moss and Whittle (2000) find that a high percentage of the circumnuclear Emission line galaxies in nearby clusters have perturbed morphologies indicative of destabilization through a tidal disturbance of some kind. Numerous studies of more distant clusters also provide strong evidence for the importance of tidal interactions and mergers. Ground-based imaging by Thompson (1988), Lavery & Henry (1988), and Lavery, Pierce, & McClure (1992) revealed numerous cases of interactions in distant clusters, a result that has been dramatically confirmed by *HST* imaging (e.g., Dressler 1994a,b; Couch et al. 1998 and references therein).

### 5.3. Triggering Mechanism for Centralized Star Formation

Finally, a key question, which remains to be addressed, is what kind of tidal (or perhaps other) disturbance triggers the centralized star formation episodes which are clearly evident in the cluster galaxies studied in this paper. Due to its presence in a ram-pressure-free environment, NGC7648 offers a particularly good perspective on this question. However, the comparison of NGC7648 with four late-stage merger candidates in §4.4 leads to inconclusive results. With its low (and likely centrally concentrated) HI content, and apparent lack of an exponential disk component, NGC7648 fails to fit in with either the equal mass or intermediate mass ratio merger scenarios. The one late-stage merger candidate with similarly low HI content, NGC4424, is resident in the Virgo cluster, and believed to be a victim of ram pressure stripping (Kenney et al. 1996). It appears that either the progenitor galaxies (perhaps low in atomic hydrogen) and/or encounter geometry must be fundamentally different from the late-stage mergers considered here, or the merger scenario might be incorrect. In that case, another type of tidal disturbance, e.g., “galaxy harassment” (Moore et al. 1996; 1998) or destabilization from the rapidly varying (sub)cluster gravitational potential (Byrd & Valtonen 1990; Bekki 1999), could supply the triggering mechanism. Unfortunately, the data presented here is not sufficient to resolve this important issue.

In conclusion, we have shown that some early-type galaxies in nearby clusters are experiencing, or have recently experienced, unusual star formation histories when compared with those in more isolated galaxies. Specifically, star formation in these galaxies is more centrally concentrated than in the disks of isolated spiral galaxies. Thus the cluster environment is clearly influencing the evolution of these galaxies. The cause of this centralized star formation is somewhat less clear. In principle it could be due to the preferential removal, by ram-pressure stripping, of the atomic gas in the galaxy’s disk, thereby allowing only for star formation in the central region. Alternatively, it may result from external tidal perturbations, which cause gas to be driven into the central region of the galaxy. The fact that in some cases there is good evidence that the star formation rate has been substantially enhanced in a recent starburst favors the tidal triggering mechanism.

We thank Riccardo Giovanelli for much advice and encouragement in obtaining and analyzing the 21 cm observations. We are also grateful to JoAnn Eder, Karen O’Neil, and the staff of the Arecibo Observatory for their help with the 21 cm observations and reductions. In addition, we thank Francois Schweizer for helpful comments regarding the morphology of NGC7648. This research was supported by NSF grant AST-9900720 to the University of North Carolina. Travel to Arecibo was partially supported by the National Astronomy and Ionosphere Center.

## REFERENCES

Abadi, M. G., Moore, B., & Bower, R. G. 1999, MNRAS, 308, 947

Balcells, M., & Peletier, R. F. 1994, AJ, 107, 135

Balogh, M. L., Morris, S. L., Yee, H. K. C., Carlberg, R. G., & Ellingson, E. 1997, ApJ, 488, L75

Baldwin, J. A., Phillips, M. M., & Terlevich, R. 1981, PASP, 93, 5

Balogh, M. L., Morris, S. L., Yee, H. K. C., Carlberg, R. G., & Ellingson, E. 1999, ApJ, 527, 54

Barger, A. J., Aragón-Salamanca, A., Ellis, R. S., Couch, W. J., Smail, I., & Sharples, R. M. 1996, MNRAS, 279, 1

Bekki, K. 1999, ApJ, 510, L15

Bender, R., Döbereiner, S., & Möllenhoff, C. 1988, A&AS, 74, 385

Bicay, M. D., Kojoian, G., Seal, J., Dickinson, D. F., & Malkan, M. A. 1995, ApJS, 98, 369

Binney, J., & Merrifield, M. 1998, Galactic Astronomy, (Princeton Univ. Press: Princeton, NJ), p. 474

Bothun, G. D., & Dressler, A. 1986, ApJ, 301, 57

Butcher, H. & Oemler, A. 1978, ApJ, 219, 18

Butcher, H. & Oemler, A. 1984, ApJ, 285, 426

Byrd, G., & Valtonen, M. 1990, ApJ, 350, 89

Caldwell, N., & Rose, J. A. 1997, AJ, 113, 492

Caldwell, N., & Rose, J. A. 1998, AJ, 115, 1423

Caldwell, N., Rose, J. A., & Dendy, K. 1999, AJ, 117, 140

Caldwell, N., Rose, J. A., Franx, M., & Leonardi, A. 1996, AJ, 111, 78

Caldwell, N., Rose, J. A., Sharples, R. M., Ellis, R. S., & Bower, R. G. 1993, AJ, 106, 473

Chincarini, G., & Rood, H. J. 1976, PASP, 88, 388

Couch, W. J., Barger, A. J., Smail, I., Ellis, R. S., & Sharples, R. M. 1998, ApJ, 497, 188

Dressler, A. 1980, ApJS, 42, 565

Dressler, A., & Gunn, J. E. 1983, ApJ, 270, 7

Dressler, A., Oemler, A., Butcher, H. R., & Gunn, J. E. 1994a, *ApJ*, 430, 107

Dressler, A., Oemler, A., Sparks, W. B., & Lucas, R. A. 1994b, *ApJ*, 435, L23

Dressler, A., Oemler, A. Jr., Couch, W. J., Smail, I., Ellis, R. S., Barger, A., Butcher, H., Poggianti, B. M., & Sharples, R. M. 1997, *ApJ*, 490, 577

Dressler, A., Smail, I., Poggianti, B. M., Butcher, H., Couch, W. J., Ellis, R. S., oemler, A. Jr. 1999, *ApJS*, 122, 51

Fabricant, D., Franx, M., & van Dokkum, P. 2000, (LANL preprint, astro-ph/0003360)

Fritze-von Alvensleben, U. & Gerhard, O. E. 1994, *A&A*, 285, 775

Gavazzi, G., Contursi, A., Carrasco, L., Boselli, A., Kennicutt, R., Scodellgio, M., & Jaffe, W. 1995, *A&A*, 304, 325

Giovanelli, R., & Haynes, M. P. 1986, *ApJ*, 292, 404

Gunn, J. E., & Gott, J. R. 1972, *ApJ*, 176, 1

Hibbard, J. E., Guhathakurta, P., van Gorkom, J. H., & Schweizer, F. 1994, *AJ*, 107, 67

Jansen, R. A., Fabricant, D., Franx, M., & Caldwell, N. 2000a, *ApJS*, 126, 271

Jansen, R. A., Fabricant, D., Franx, M., & Caldwell, N. 2000b, *ApJS*, 126, 331

Jogee, S., Kenney, J. D. P., & Smith, B. J. 1999, *ApJ*, 526, 665

Kenney, J. D. P., & Koopmann, R. A. 1999, *AJ*, 117, 181

Kenney, J. D. P., Koopmann, R. A., Rubin, V. C., & Young, J. S. 1996, *AJ*, 111, 152

Kodama, T., & Bower, R. G. 2000, (LANL preprint, astro-ph/0005397)

Lavery, R. J., & Henry, J. P. 1988, *ApJ*, 330, 596

Lavery, R. J., Pierce, M. J., & McClure, R. D. 1992, *AJ*, 104, 2067

Koopmann, R. A., & Kenney, J. D. P., 1998, *ApJ*, 497, L75

Margoniner, V. E., & de Carvalho, R. R. 2000, *AJ*, 119, 1562

Moore, B., Katz, N., Lake, G., Dressler, A., & Oemler, A. 1996, *Nature*, 379, 613

Moore, B., Lake, G., & Katz, N. 1998, *ApJ*, 495, 139

Moss, C., & Whittle, M. 1993, *ApJ*, 407, L17

Moss, C., & Whittle, M. 2000, *MNRAS*, 317, 667

Newberry, M. V., Boroson, T. A., & Kirshner, R. P. 1990, *ApJ*, 350, 585

Peletier, R. F., Davies, R. L., Illingworth, G. D., Davis, L. E., & Cawson, M. 1990, *AJ*, 100, 1091

Poggianti, B. M., Smail, I., Dressler, A., Couch, W. J., Barger, A., Butcher, H., Ellis, R. S., & Oemler, A. Jr. 1999, *ApJ*, 518, 576

Quilis, V., Moore, B., & Bower, R. 2000, (LANL preprint, astro-ph/0006031)

Rubin, V. C., Waterman, A. H., & Kenney, J. D. P. 1999, AJ, 118, 236

Schweizer, F. 1982, ApJ, 252, 455

Schweizer, F. 1996, AJ, 111, 109

Smith, B. J. 1994, AJ, 107, 1695

Thompson, L. 1988, ApJ, 324, 112

Vader, J. P., Vigroux, L., Lachieze-Rey, M., & Souviran, J. 1988, A&A, 203, 217

Vigroux, L., Boulade, O., & Rose, J. A. 1989, AJ, 98, 2044

Zwicky, F., Herzog, E., & Wild, P. 1961-1968, “Catalog of Galaxies and Clusters of Galaxies”,  
(Pasadena; California Institute of Technology)



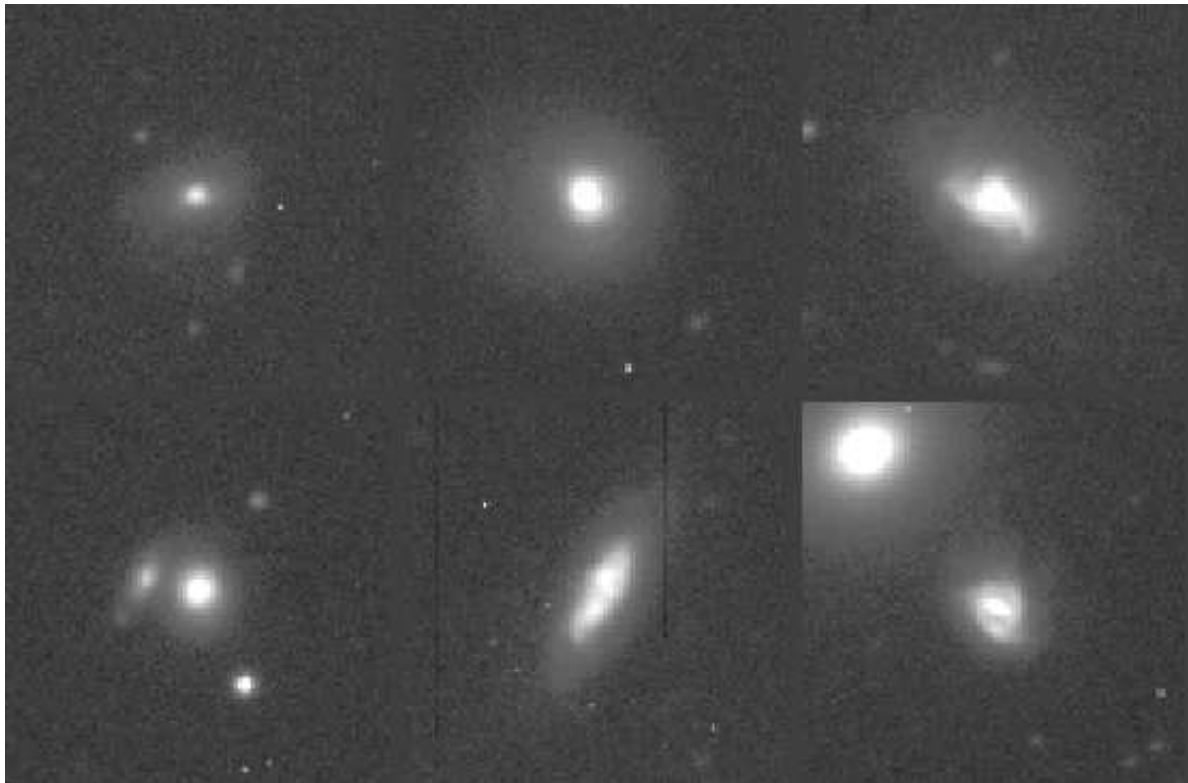


Fig. 1.— V bandpass images of four of the BD86 spirals are compared with images of the early-type galaxies Coma D-15 and D-45 (lower left and top left panels, respectively). The BD86 spirals are D54 and D169 (middle upper and lower panels) and D51 and D195 (upper and lower right panels). In contrast to the BD86 spirals, the star formation in D15 and D45 is taking place in what appears to be the bright central “bulges” of these galaxies.

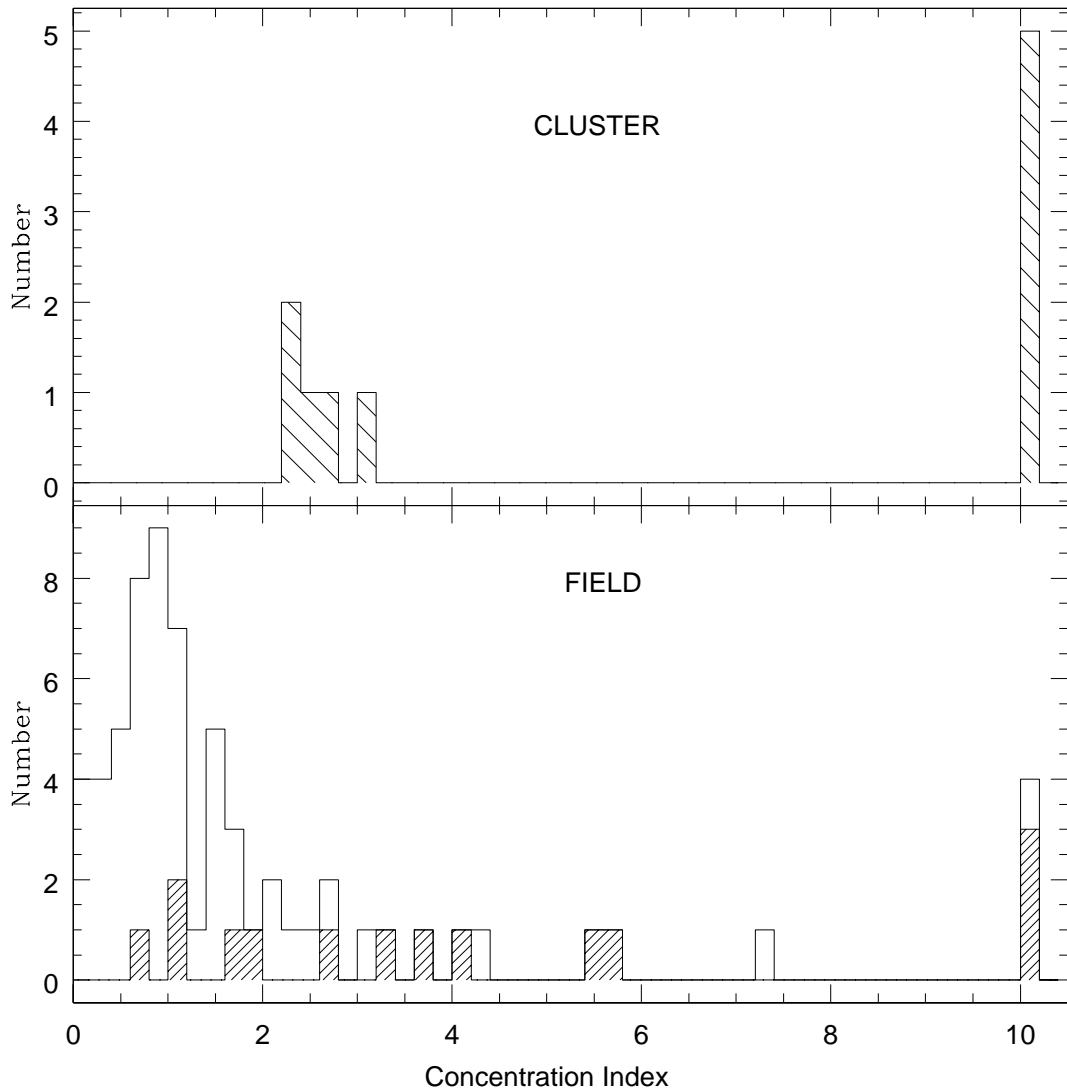


Fig. 2.— The histogram of the C/R ratios of the cluster emission-line early-type galaxies (top) is compared with that of the NFGS galaxies (bottom). The shaded part of the NFGS histogram represents those galaxies which have been classified as Markarian, interacting, starburst, etc.

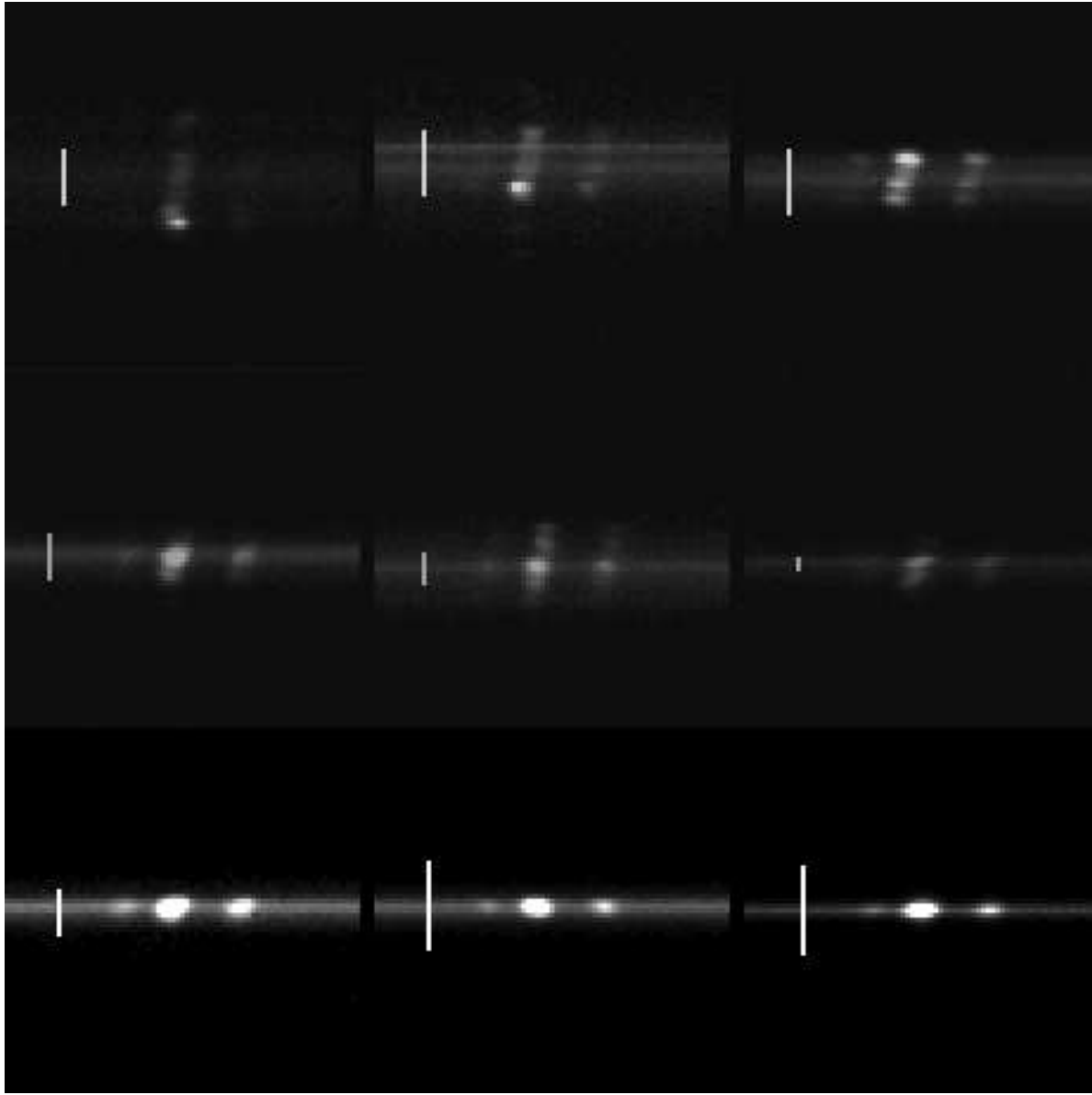


Fig. 3.— Mosaic of long-slit spectra of NFGS galaxies. Top panels contain representative galaxies with low central concentration emission lines, i.e., with  $C/R < 2$ . Middle panels contain galaxies with intermediate central concentration emission lines, i.e., with  $2 \leq R \leq 4$ . The bottom panels show galaxies with high central concentration emission, i.e., with  $R > 4$ . The fiducial line for each spectrum is 4 kpc long.

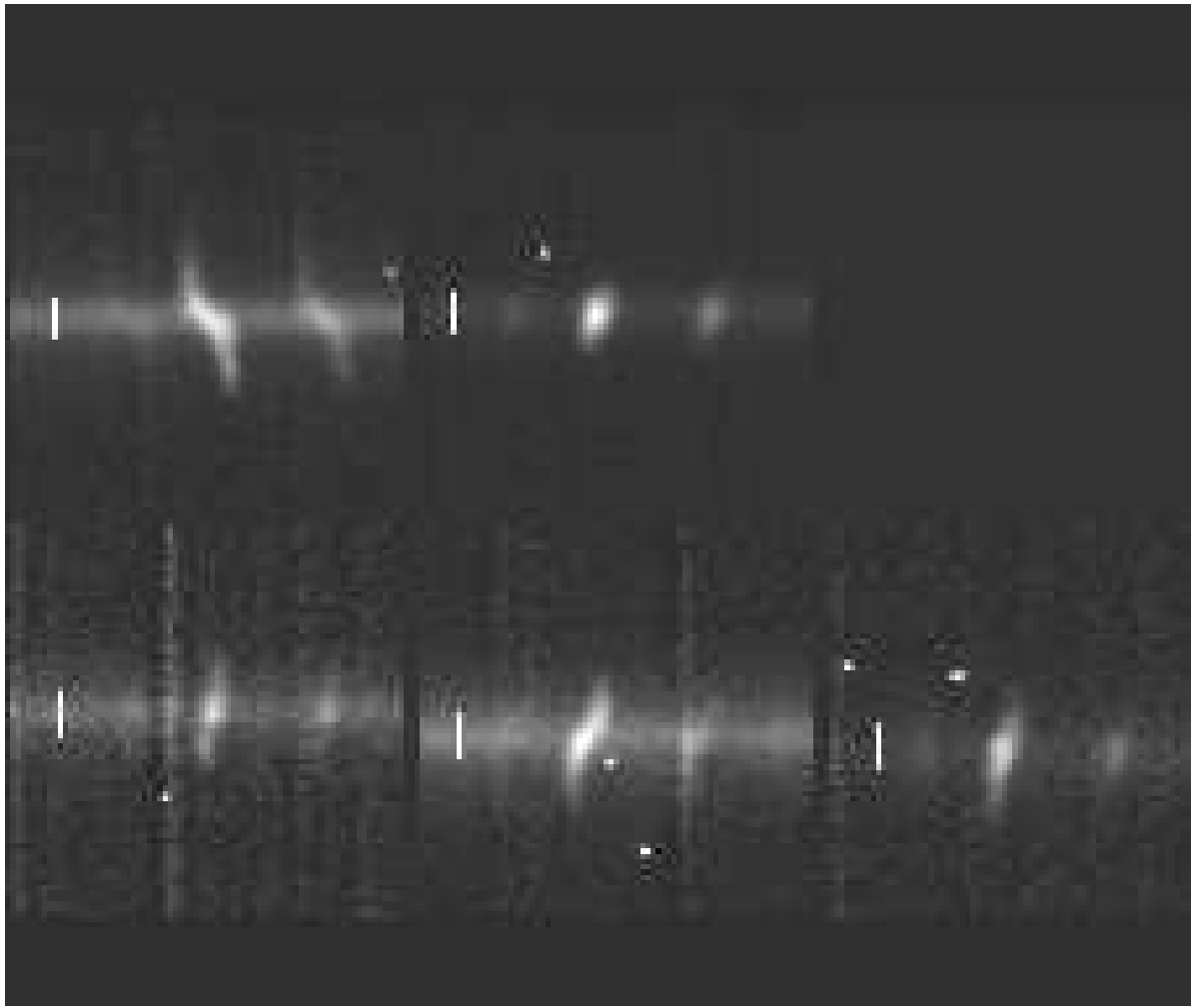


Fig. 4.— Mosaic of long-slit spectra of cluster galaxies with intermediate concentration emission lines. The fiducial line for each spectrum is 4 kpc long.

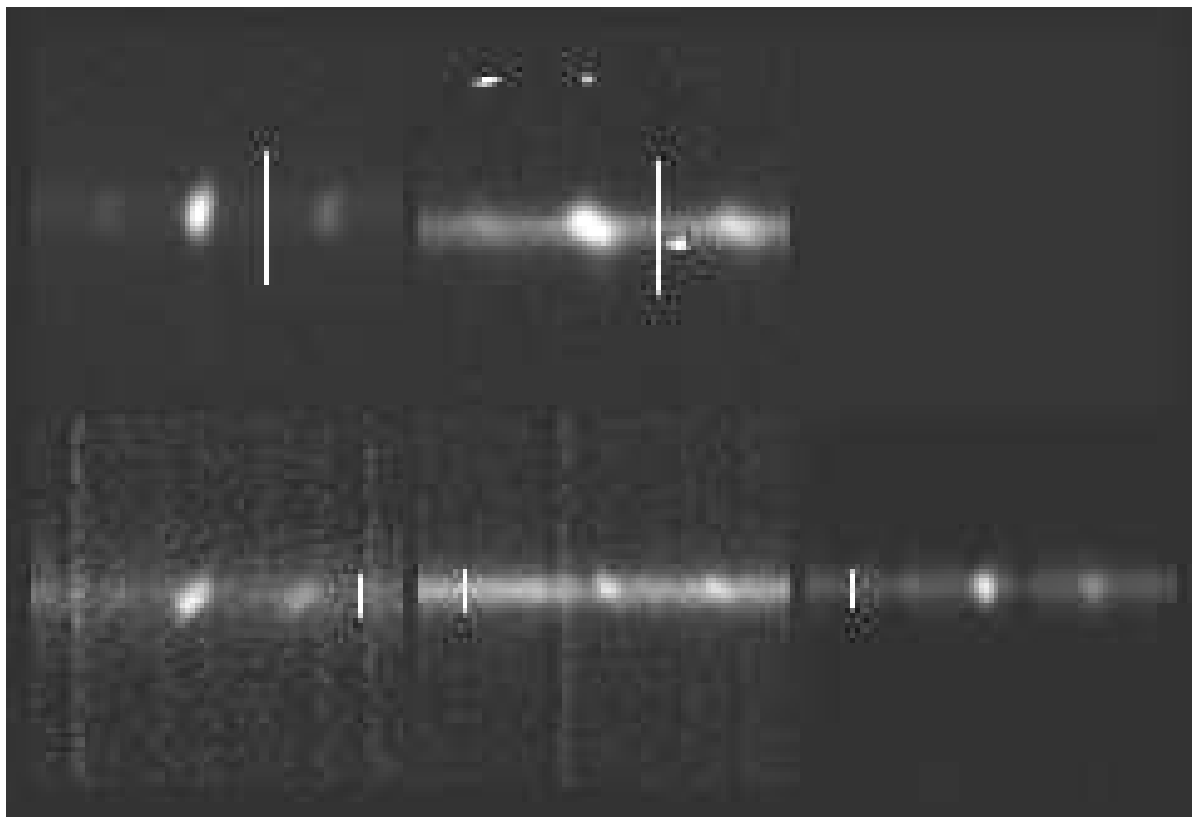


Fig. 5.— Mosaic of long-slit spectra of cluster galaxies with high concentration emission lines. The fiducial line for each spectrum is 4 kpc long.

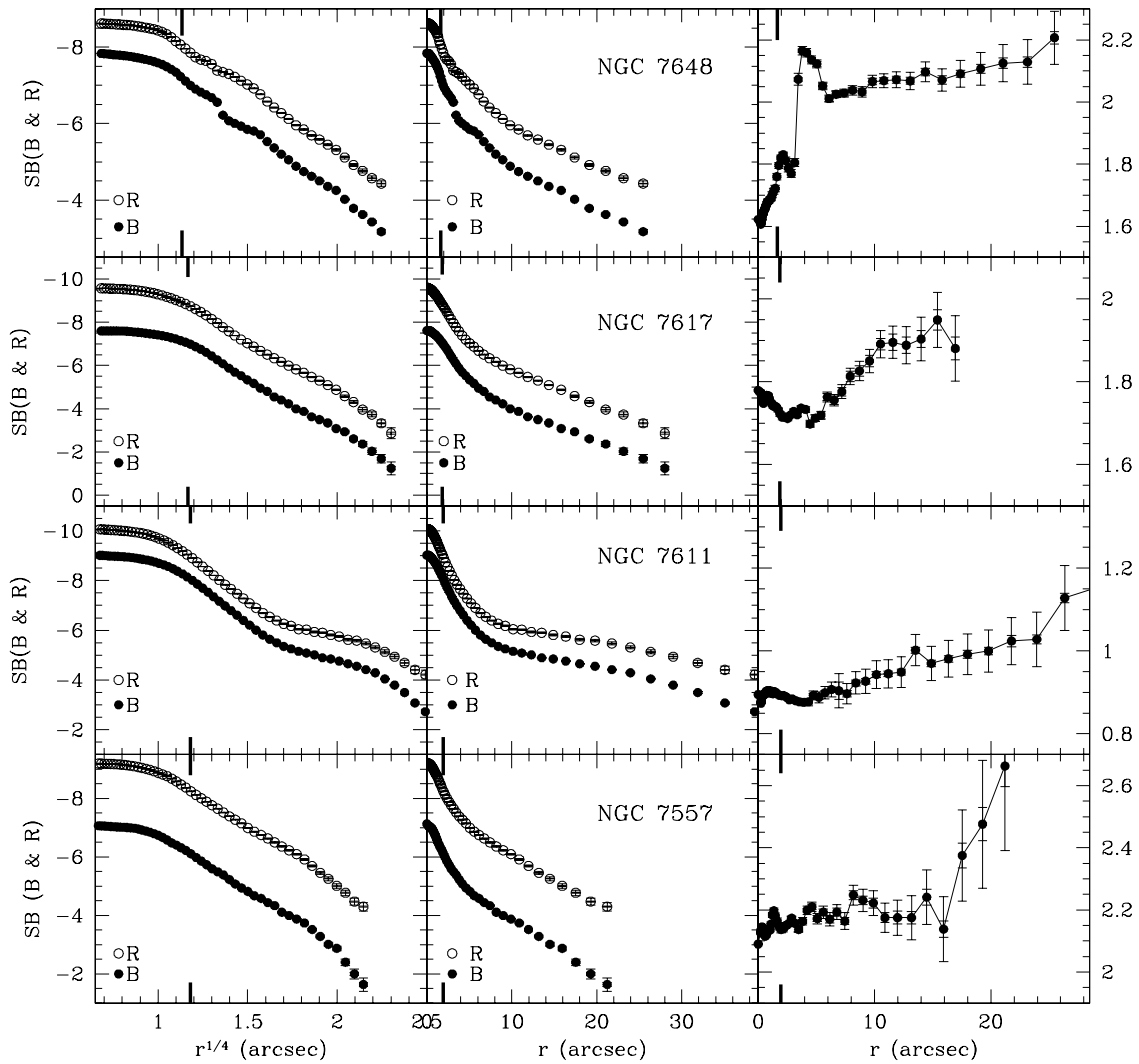


Fig. 6.— Azimuthally averaged radial luminosity and color profiles are plotted for the four Pegasus I early-type galaxies. The radial B and R profiles are plotted versus both  $r^{1/4}$  and  $r$  in the left and center panels, respectively, while the  $\Delta(B - R)$  color profiles are shown in the right panels. The thick solid lines marked on the horizontal axis indicate the seeing size (FWHM). The two sets of error bars indicate the statistical errors and the errors calculated from estimated uncertainties in sky subtraction (see text); the latter errors dominate at larger radii.

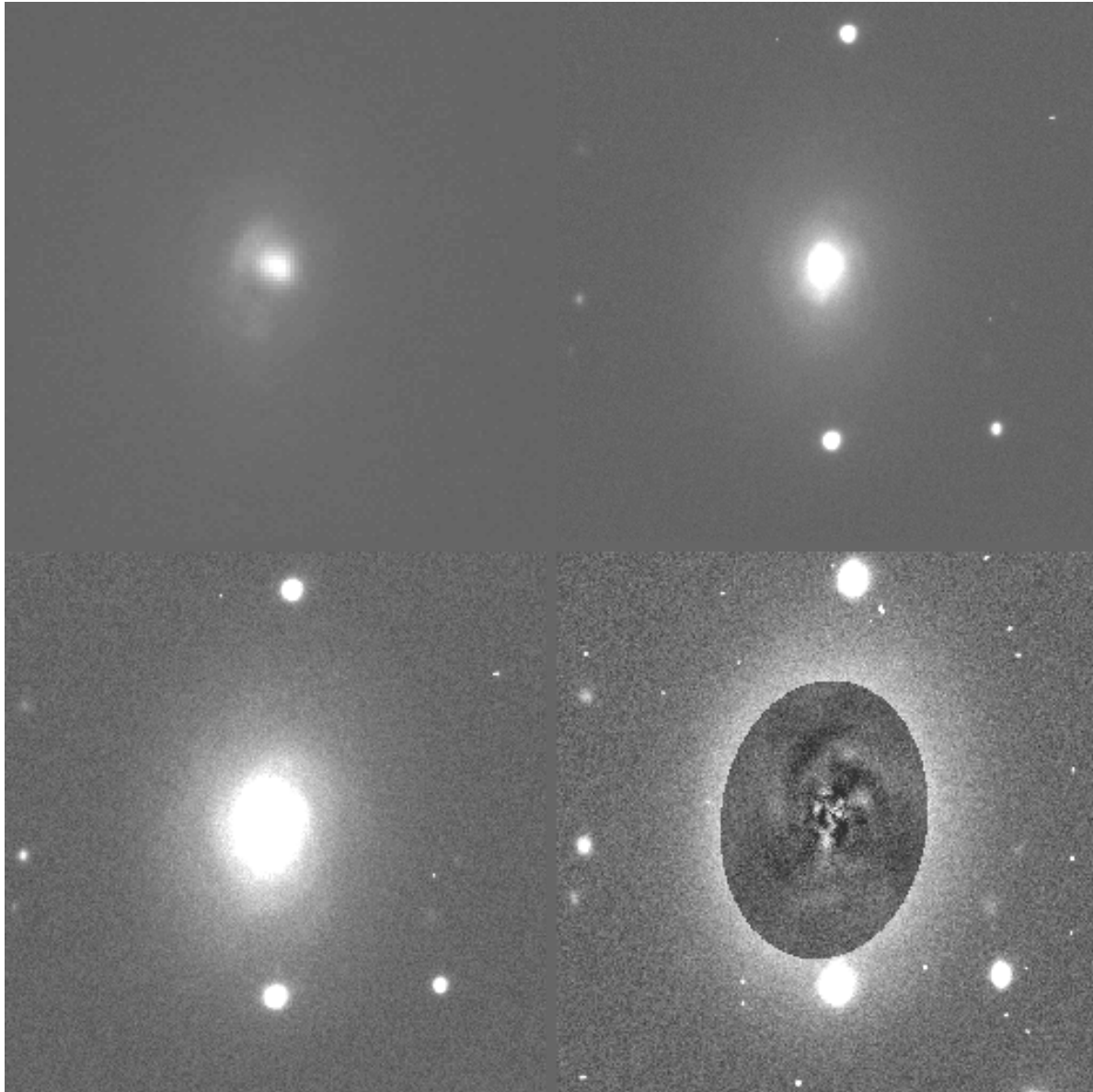


Fig. 7.— Mosaic of images of NGC7648. Top left (a) is a B band image showing only the structure in the central region. It is displayed at twice the scale of (b) - (d). Top right (b) is an R band image, at intermediate contrast. The separation of the two bright stars is  $\sim 80''$ . Bottom left (c) is the same R band image, at higher contrast to emphasize fainter features. Bottom right (d) is the model-subtracted version of the R band image, which emphasizes fine structure at all brightness levels. In all four panels, North is to the left, and East is to the bottom.

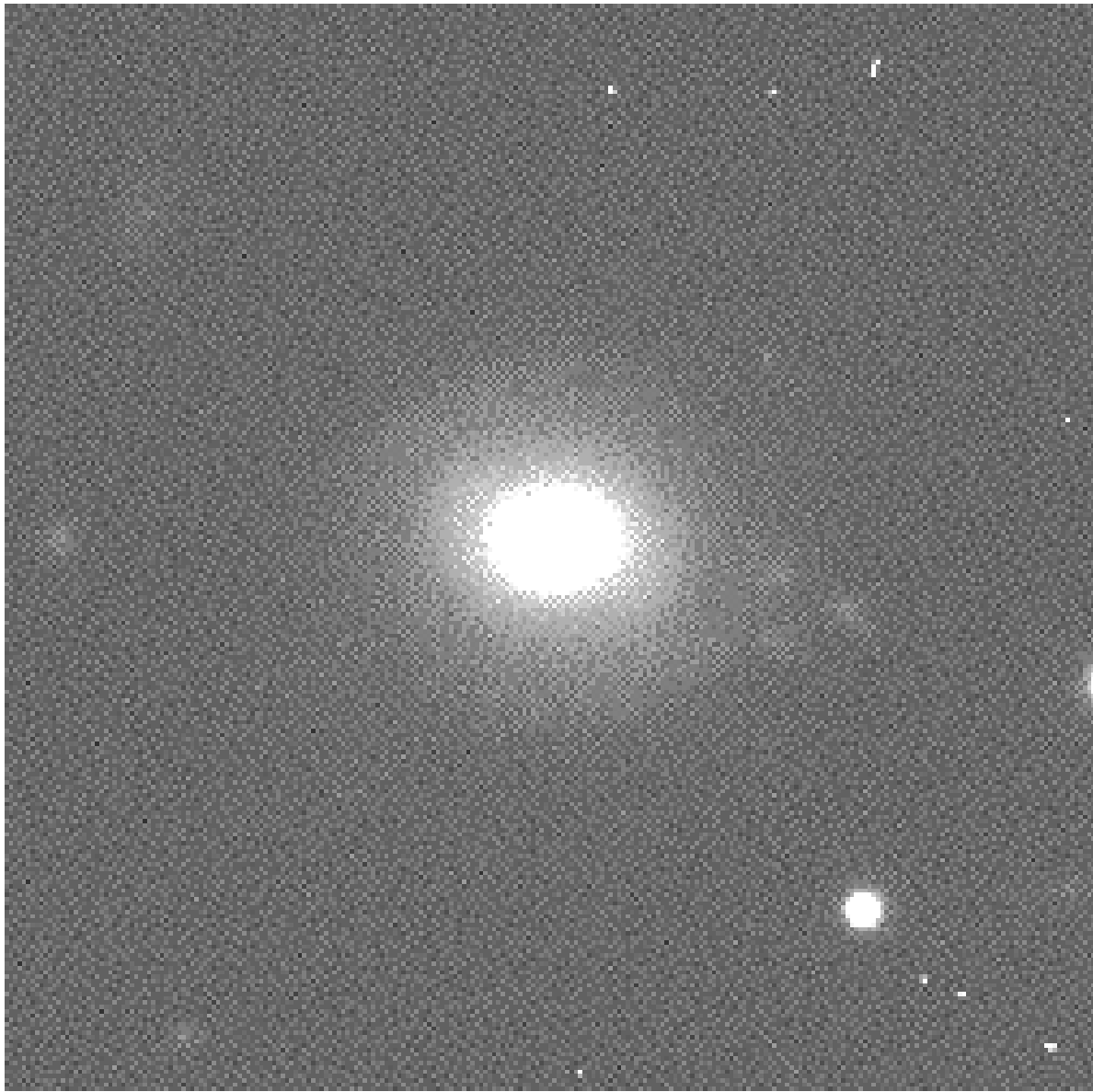


Fig. 8.— R band image of NGC7557. North is to the left, and East is to the bottom.

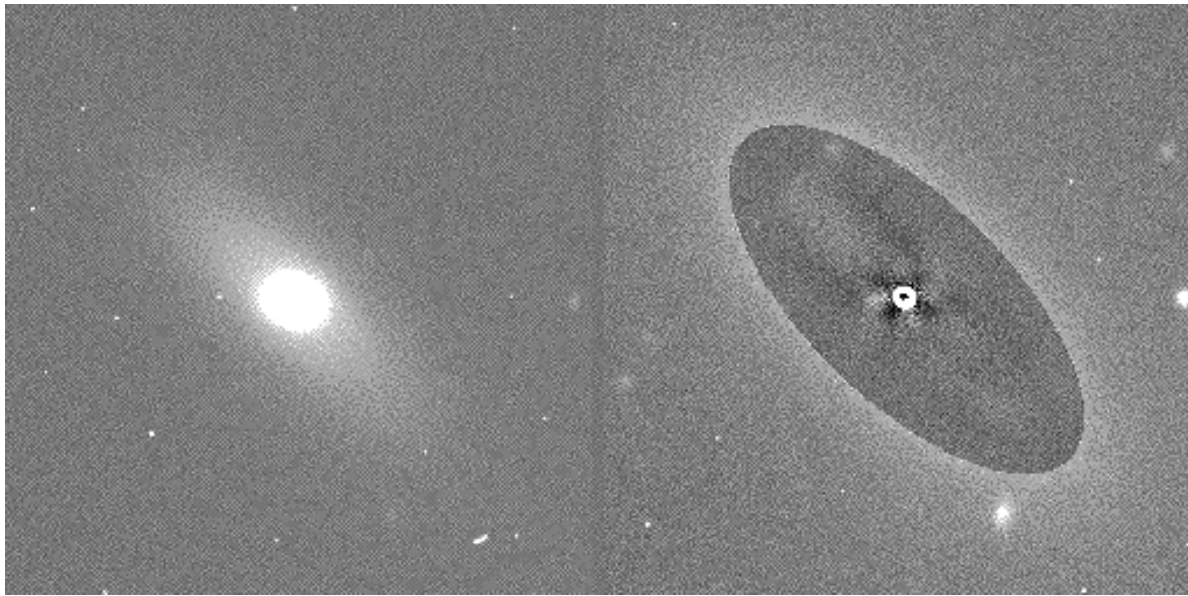


Fig. 9.— R band images of NGC7611. On the left (a) is a sky subtracted image. On the right (b) is the “fine structure” image for a deeper exposure, for which the few central pixels are saturated, thereby creating a central artifact. The bisymmetric features are seen just outside the nucleus. North is to the left, and East is to the bottom.



Fig. 10.— Left (a) and right (b) are the B and R band images of NGC7617. The curving dust lane can be seen to the north and west of the galaxy. North is to the left, and East is to the bottom.

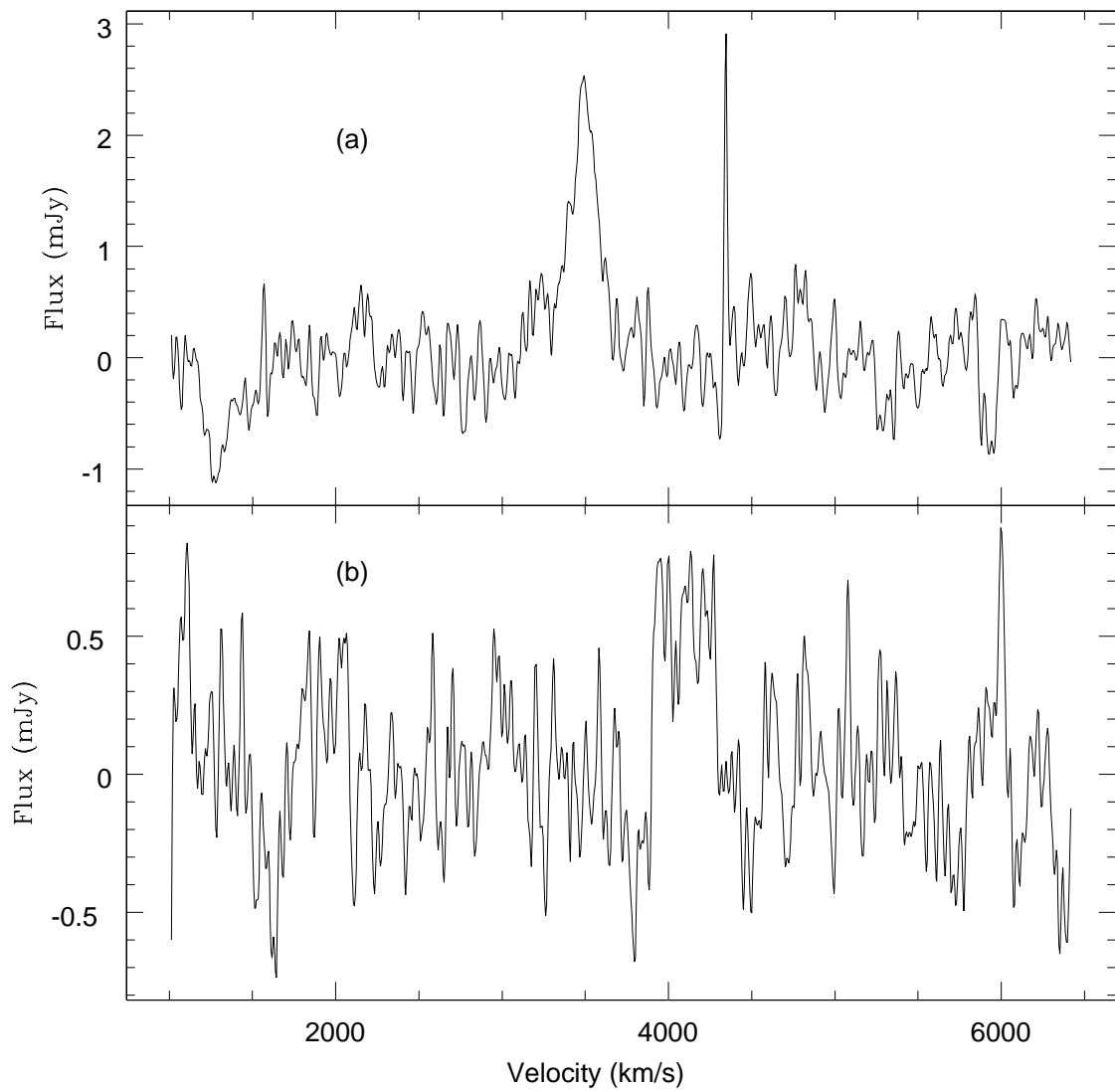


Fig. 11.— 21 cm spectral observations of (a) NGC7648 and (b) NGC7617 obtained with the Arecibo radiotelescope.

Table 1. C/R Values for Field Galaxy Sample

Galaxy ID	T	$V_r$	$M_B^1$	$r_{eff}$	C/R	Comment <sup>2</sup>
A00289+0556	7	2207	-18.00	9.52	0.95	
A00389-0159	1	5417	-20.65	11.13	4.39	
A00442+3224	3	5079	-20.34	13.08	1.73	a,b
A01344+2838	4	7934	-20.63	6.90	0.79	a
A01346+0438	4	3257	-18.54	5.08	1.65	
A02056+1444	3	4516	-20.07	11.02	2.42	a
A02257-0134	8	1795	-17.91	19.32	0.54	a
A08567+5242	3	9092	-21.63	16.70	<0.62	a
A09579+0439	3	4008	-19.05	7.95	1.55	
A10171+3853	9	1999	-17.83	7.95	0.93	a
A10321+4649	5	3372	-18.81	6.66	10.7	
A10337+1358	6	2869	-18.64	11.06	0.86	a
A10504+0454	5	5631	-19.93	4.54	5.41	b
A10592+1652	4	2830	-18.25	10.83	0.76	a
A11040+5130	5	2269	-18.99	28.02	0.40	a
A11072+1302	5	12623	-21.43	5.72	3.30	a,b
A11310+3254	3	2603	-18.49	9.98	0.88	a
A11332+3536	-3	1596	-17.44	6.40	2.66	b
A11372+2012	5	10891	-21.65	7.58	0.15	a
A11531+0132	5	1748	-18.42	33.62	1.44	a
A12001+6439	-2	1586	-17.45	8.59	5.70	b
A12167+4938	5	3720	-19.28	13.13	1.46	a
A12331+7230	3	7134	-20.41	9.69	2.28	a
A13065+5420	3	2581	-18.28	12.16	0.35	a
A13194+4232	6	3478	-18.93	10.18	2.74	a
A13361+3323	9	2420	-18.29	14.28	10.90	b
A13422+3526	4	2570	-18.17	10.58	1.17	a
A14305+1149	5	2246	-18.35	11.16	0.39	a
A15314+6744	5	6675	-20.50	13.72	0.95	a
A15523+1645	5	2290	-17.49	4.89	1.05	a,b
A22306+0750	5	2212	-18.17	7.65	0.77	
A22551+1931	-2	5926	-18.97	4.54	4.09	b
A23176+1541	7	4604	-19.64	10.79	0.17	a
A23542+1633	10	1997	-17.98	18.04	0.76	a
IC1100	6	6758	-20.72	10.04	0.78	a
IC1124	2	5346	-19.85	7.30	1.30	a



Table 1—Continued

Galaxy ID	T	$V_r$	$M_B^1$	$r_{eff}$	C/R	Comment <sup>2</sup>
IC1776	5	3486	-19.39	19.72	0.70	a
IC197	4	6401	-20.31	7.90	0.62	a,b
IC2591	4	6731	-20.48	8.97	1.51	a
IC746	3	4989	-19.53	7.80	0.54	
NGC2780	2	1916	-17.66	12.11	7.23	
NGC3009	5	4682	-19.46	11.37	2.18	
NGC3326	3	7972	-20.91	7.49	19.06	b
NGC3633	1	2398	-18.22	7.49	3.10	
NGC4034	5	2542	-18.41	20.09	0.06	a
NGC4120	5	2411	-18.42	15.85	1.03	a
NGC4141	5	2098	-18.75	11.25	0.93	a
NGC4159	8	1945	-17.96	11.56	0.94	a
NGC4238	5	2910	-18.83	13.01	1.72	a
NGC4961	4	2545	-19.06	12.68	0.90	a
NGC5117	5	2436	-18.41	16.38	1.10	a
NGC5230	5	6829	-21.74	22.91	2.12	a
NGC5267	3	6021	-20.57	11.49	0.60	a
NGC5425	5	2189	-18.25	12.49	0.57	a
NGC5491	5	5818	-20.68	11.81	0.18	a
NGC5541	5	7804	-21.29	9.01	0.35	a
NGC5762	1	1817	-18.11	11.44	0.93	a
NGC5874	4	3309	-19.70	26.14	0.26	a
NGC5875A	5	2645	-18.37	11.10	1.03	a
NGC5993	3	9747	-21.73	11.08	0.55	a
NGC6007	4	10629	-21.86	14.33	1.40	a
NGC6131	5	5241	-20.13	15.84	1.18	a
NGC695	5	9855	-21.76	6.33	1.86	a,b
NGC7328	2	3051	-19.37	13.23	10.81	
NGC7620	6	9811	-21.93	8.42	1.17	b

<sup>1</sup>Based on the total B magnitude given in Jansen et al. (2000a), and  $H_0 = 70 \text{ km s}^{-1} \text{ Mpc}^{-1}$

<sup>2</sup>a: used the C/B value in place of C/R; b: known to be a Markarian, starburst, or interacting galaxy, etc. from information given in NED

Table 2. C/R Values for Cluster Early-Type Galaxy Sample

Galaxy ID	T	$M_B$ <sup>a</sup>	$r_{eff}$	C/R
DC2048#104	S0/a	—	3.0 <sup>b</sup>	13.47
DC2048#148	S0	-18.93	3.4	2.70
DC2048#172	S0/a	-18.76	3.2	3.01
DC2048#192	E	-19.53	3.0	10.90
DC2048#187	S0	-18.85	3.8	2.56
DC0326#82a	E	-19.18	3.0	26.96
DC0326#101a	S0/a	-19.32	2.8	2.26
DC0326#80b	E	-18.92	2.0	2.37
Coma-D45	Sa	-18.28	4.0	106.10
Coma-D15	S0	-18.97	4.0	24.10

<sup>a</sup>Based on the total B magnitude given in Caldwell et al. (1993), or Caldwell & Rose (1997), and  $H_0 = 70 \text{ km s}^{-1} \text{ Mpc}^{-1}$

<sup>b</sup>No data available – assumed a value of 3.0, based on other galaxies in the cluster

Table 3. 21 cm Data for Pegasus I and Coma Galaxies

Galaxy ID	Detected Flux (Jy km/s)	$3\sigma$ Noise (Jy km/s)	$M_{HI}$ ( $M_\odot$ )	$M_B$	$M_{HI}/L_B$ ( $M_\odot/L_\odot$ )
NGC7557	...	0.27	$<2.0 \times 10^8$	-18.87	$<4.3 \times 10^{-2}$
NGC7611	...	0.15	$<1.3 \times 10^8$	-20.50	$<5.3 \times 10^{-3}$
NGC7617	0.21	0.10	$1.7 \times 10^8$	-19.24	$2.3 \times 10^{-2}$
NGC7648	0.46 <sup>a</sup>	0.14	$3.9 \times 10^8$	-20.25	$2.0 \times 10^{-2}$
...	0.56 <sup>a</sup>	0.14	$4.8 \times 10^8$	-20.25	$2.5 \times 10^{-2}$
Coma-D15	0.088	0.080	$2.1 \times 10^8$	-18.97	$3.6 \times 10^{-2}$
Coma-D16	...	0.080	$<1.9 \times 10^8$	-18.86	$<3.6 \times 10^{-2}$
Coma-D45	...	0.079	$<1.8 \times 10^8$	-18.28	$<5.8 \times 10^{-2}$
Coma-D100	0.043 <sup>b</sup>	0.076	$1.0 \times 10^8$	-19:	$1.7 \times 10^{-2}$
...	...	0.076	$<1.8 \times 10^8$	-19:	$<3.0 \times 10^{-2}$

<sup>a</sup>The lower and upper values correspond to when the wings on the 21 cm profile are not and are included, respectively.

<sup>b</sup>The first line for Coma-D100 corresponds to results from an assumed  $1.7\sigma$  detection; the second line corresponds to the  $3\sigma$  upper limit.

Table 4. Physical Parameters for Merging Galaxies<sup>a</sup>

Galaxy ID	Tidal Tails?	Exponential Disk?	$M_{HI}/L_B$ ( $M_\odot/L_\odot$ )	log [L(FIR)/ $L_\odot$ ] <sup>b</sup>	log f12/f25	log f25/f60	log f60/f100	log P(1.415 [W/Hz])
NGC3921	y	n	0.09	...	...	-0.88	...	...
NGC7252	y	n	0.07	10.65	-0.26	-0.96	-0.25	...
NGC2782	y	y	0.13	10.84	-0.30	-0.79	-0.23	21.74
NGC4424	n	y	0.03	9.38	-0.30	-0.96	-0.25	<20.2
NGC7648	n	n	0.02	10.47	-0.41	-0.95	-0.20	21.62

<sup>a</sup>all values taken from the literature have been rescaled to  $H_0 = 70 \text{ km s}^{-1} \text{ Mpc}^{-1}$

<sup>b</sup>The far-infrared (FIR) luminosity is as defined in Table 5 of Bicay et al. (1995)